PCCP

RSC Publishing

PAPER

View Article Online
View Journal | View Issue

Cite this: *Phys. Chem. Chem. Phys.*, 2013, **15**, 1115

Ultrafast dynamics in iron tetracarbonyl olefin complexes investigated with two-dimensional vibrational spectroscopy†

Matthijs R. Panman, Arthur C. Newton, Jannie Vos, Bart van den Bosch, Vladica Bocokić, Joost N. H. Reek* and Sander Woutersen*

The dynamics of iron tetracarbonyl olefin complexes has been investigated using two-dimensional infrared (2D-IR) spectroscopy. Cross peaks between all CO-stretching bands show that the CO-stretch modes are coupled, and from the cross-peak anisotropies we can confirm previous assignments of the absorption bands. From the pump–probe delay dependence of the diagonal peaks in the 2D-IR spectrum we obtain a correlation time of $\sim$3 ps for the spectral fluctuations of the CO-stretch modes. We observe a multi-exponential pump–probe delay dependence of the cross-peak intensities, with rate constants ranging from 0.1 ps^{-1} to 0.6 ps^{-1}. To determine whether this delay dependence originates from fluxionality of the complex or from intramolecular vibrational relaxation (IVR), we modulate the free-energy barrier of fluxional rearrangement by varying the pi-backbonding capacities of the olefin ligand in two iron tetracarbonyl olefin complexes: $Fe(CO)_4$(cinnamic acid) and $Fe(CO)_4$(dimethyl fumarate). Since the pi-backbonding strongly influences the rate of fluxionality, comparing the dynamics in the two complexes allows us to determine to what extent the observed dynamics is caused by fluxionality. We conclude that on the time scale of our experiments (up to 100 ps) the cross-peak dynamics in the iron complexes is determined by intramolecular vibrational energy relaxation. Hence, in contrast to previously investigated irontricarbonyl and ironpentacarbonyl complexes, iron tetracarbonyl olefin complexes exhibit no fluxionality on the picosecond time scale.

Received 9th October 2012,
Accepted 27th November 2012

DOI: 10.1039/c2cp43565a

www.rsc.org/pccp

1 Introduction

Fluxionality, the rapid rearrangement of a molecule between two conformations, is a process that occurs in many transition-metal complexes. Penta-coordinated systems are well known for fluxional behavior as the energy barrier between trigonal bipyramidal and square pyramidal geometries is often quite low. Established examples of fluxionality include the Berry pseudo-rotation in $Fe(CO)_5$, PF_5, and the ring rotation in ferrocene. Such conformational flexibility is of importance for understanding chemical reactivity, as it affects the stereoselectivity of many organic, inorganic, and organometallic reactions.[1] Moreover, fluxionality constitutes an elementary example of a chemical reaction. In transition-metal complexes that contain CO ligands, fluxionality can be investigated conveniently by probing the CO-stretch response using infrared spectroscopy. This is because the CO ligands are permuted during a fluxional rearrangement. Consequently, if there are IR-active normal modes in which the contributions of the stretching motions of the CO ligands are not identical, a rearrangment of the CO ligands in which the vibrational excitations of the individual CO ligands are preserved leads to a redistribution of the excitation between these normal modes. This redistribution is observed as an exchange of vibrational excitations between the normal modes.[2] If the fluxionality occurs on a time scale comparable to the inverse of the frequency difference between the normal modes (typically 10–100 cm^{-1}, corresponding to 0.1–1 ps), the resulting energy redistribution can be investigated by analysis of coalescence lineshapes in the vibrational spectrum, in a manner similar to the analysis of nuclear-magnetic resonance (NMR) coalescence lineshapes,

Van't Hoff Institute for Molecular Sciences, University of Amsterdam, Science Park 904, 1098 XH Amsterdam, The Netherlands. E-mail: s.woutersen@uva.nl, j.n.h.reek@uva.nl; Fax: +31 20 525 6965; Tel: +31 525 7091

† Electronic supplementary information (ESI) available: Delay scans for delay times up to 150 ps and a least-squares fit to determine T_1; singular-value decomposition of the delay-dependent $Fe(CO)_4$(cinnamic acid) and $Fe(CO)_4$(dimethyl fumarate) data; singular value decomposition of the delay-dependent intensity of the cross peaks of the $Fe(CO)_4$(cinnamic acid) and $Fe(CO)_4$(dimethyl fumarate) 2D-IR spectra. See DOI: 10.1039/c2cp43565a

but on a time scale that is many orders of magnitude faster.[3–6] For processes that occur on a slower time scale, such an analysis generally becomes difficult.

It has recently become clear that two-dimensional vibrational spectroscopy[7–10] is a much more generally applicable and powerful method to investigate dynamical processes in transition-metal complexes.[2,11–19] In particular, experiments in which conformational exchange and vibrational excitation transfer are observed in the time domain have now become possible. In these experiments, one resonantly excites a specific normal mode of a particular conformation, and by probing the other normal modes as a function of the time delay with respect to the initial excitation, one can observe the rate at which energy is exchanged between the normal modes. In a two-dimensional vibrational spectrum, this process is observed as the appearance of off-diagonal peaks with increasing delay (waiting time) between the excitation and probe pulses.[20–23]

A redistribution of the CO-stretch vibrational excitation can be caused by a fluxional rearrangement of the CO ligands, but can also originate from equilibration of the vibrational excitation over the normal modes (intramolecular vibrational relaxation or IVR). If the normal modes are strongly coupled, such an equilibration process can take place on a picosecond time scale.[12,24–26] In previous studies where ultrafast redistribution of CO-stretch excitations was observed, several approaches were used to determine by which process (fluxionality or IVR) it was caused. In particular, the dependence of the observed energy redistribution rate on temperature[2,18] and viscosity[27] can be used for this purpose.

Here, we investigate vibrational CO-stretch cross-peak dynamics by modulating the free-energy barrier of fluxionality in pentacoordinated iron complexes with four carbonyl and one olefin ligand. Previous work has shown that the fluxionality in both tricarbonyl-iron[5,6] and pentacarbonyl-iron[2,17–19] complexes occurs on the picosecond and subpicosecond time scale. The fluxional behavior in tetracarbonyl complexes might be expected to occur on a similar time scale. Iron tetracarbonyl olefin complexes exhibit four infrared-active modes, and this provides an elegant way to distinguish the contributions of fluxionality and IVR to the observed cross-peak dynamics. Since fluxionality is characterized by a single rate constant, all observed excitation transfer rates should be identical if the energy redistribution is caused by fluxionality only. Deviations from this situation must be due (at least in part) to IVR. In addition, by coordinating different olefin ligands to the iron, the electronic properties of the complex can be tuned so as to modify the free-energy barrier for the fluxional motion, and thereby the contribution of fluxionality to the cross-peak dynamics.

2 Experiment

Using an experimental setup which has been described previously,[28] we generate mid-infrared pulses with a duration of $\sim$50 fs at 2000 cm^{-1}, and an energy and a bandwidth of 10 μJ and $\sim$300 cm^{-1}, respectively. A small fraction of the mid-infrared pulses is split off to obtain broad-band probe pulses. The remainder is passed through an infrared Fabry–Perot filter, resulting in pump pulses with a bandwidth of 10 cm^{-1} and an energy of approximately 1 μJ, the center frequency of which is varied by adjusting the Fabry–Perot filter using piezo-electric controllers. The pump pulses have an intensity envelope that is approximately single-sided exponential with a FWHM of 800 fs, as determined from a cross correlation measured using two-photon absorption in InAs placed in a sample cell identical to the one used in the experiments on the samples containing the solutions of the Fe-complex. Transient absorption changes ΔA are measured by frequency-dispersed detection of the probe and reference pulses using a 2×32 mercury–cadmium–telluride detector array. The anisotropies R of the signals are determined by repeatedly performing the measurements with parallel and perpendicularly polarized pump and probe pulses, and calculating $R = (\Delta A_{\parallel} - \Delta A_{\perp})/(\Delta A_{\parallel} + 2\Delta A_{\perp})$.

Two Fe-complexes, $Fe(CO)_4$(cinnamic acid) and $Fe(CO)_4$(dimethyl fumarate), were prepared as described previously[29] from compounds purchased from Sigma-Aldrich. All experiments were carried out on 1.81×10^{-3} M solutions of either complex in $CDCl_3$. The samples were kept in a sealed IR-cell equipped with 3 mm CaF_2 windows separated by a 500 μm spacer.

3 Results and discussion

3.1 Absorption spectra and normal modes of the complexes

The investigated complexes are shown in Fig. 1A and B. In $Fe(CO)_4$(olefin) complexes, the olefin ligand is equatorially coordinated, and the $Fe(CO)_4$ moiety of the complexes has

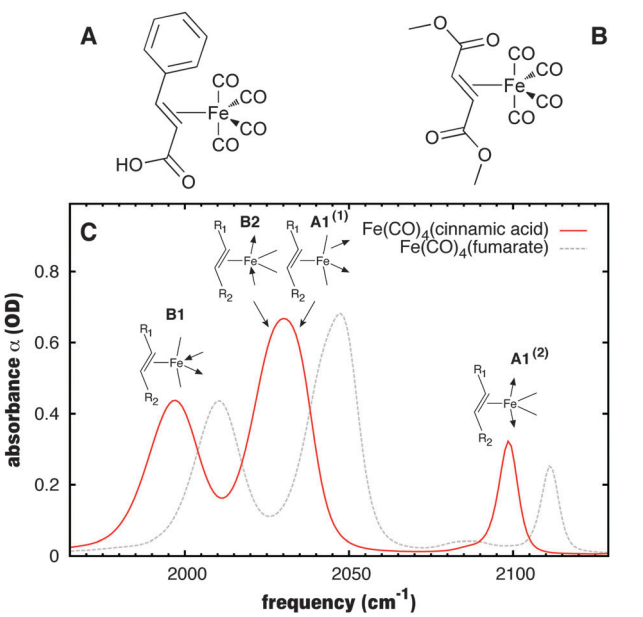

Fig. 1 (A) Chemical structure of $Fe(CO)_4$(cinnamic acid). (B) Chemical structure of $Fe(CO)_4$(dimethyl fumarate). (C) Infrared absorption spectra of the complexes. The CO-stretching motions of the normal modes associated with each of the absorption bands have been indicated schematically. The band in the middle arises from two overlapping absorption bands.

approximate C_{2v} symmetry.[30] There are four CO-stretching modes, with symmetries $A_1^{(1)}$, $A_1^{(2)}$, B_1 and B_2 (shown schematically in Fig. 1C), which are all infrared-active. The energy order of these four modes (also indicated in the figure) has been determined previously from a normal-mode analysis of the IR absorption spectra combined with ^{13}C-isotope labeling.[31] In the experimental IR spectra of $Fe(CO)_4$(cinnamic acid) and $Fe(CO)_4$-(dimethyl fumarate) shown in Fig. 1, the B_2 and $A_1^{(1)}$ absorption bands overlap, and only three bands can be distinguished. With cinnamic acid as the olefin ligand, these bands are at frequencies of approximately 1998 cm^{-1} (B_1 mode), 2030 cm^{-1} (B_2 and $A_1^{(1)}$ modes), and 2100 cm^{-1} ($A_1^{(2)}$ mode). With dimethyl fumarate as the ligand, essentially the same spectrum is observed, apart from an overall 10 cm^{-1} frequency increase of all the CO-stretch modes. This difference is due to the stronger π-backbonding to the dimethyl-fumarate as compared to the cinnamic-acid complex. This leads to stronger C≡O bonds, and thus higher CO-stretching frequencies in the $Fe(CO)_4$(dimethyl fumarate) as compared to the $Fe(CO)_4$(cinnamic acid) complex.

3.2 2D-IR spectrum

Fig. 2 shows the 2D vibrational spectrum of $Fe(CO)_4$(cinnamic acid) for several delays after vibrational excitation. In this 2D graph, the absorption change $\Delta\alpha$ is plotted as a function of the pump and probe frequencies, with positive $\Delta\alpha$ denoted by red colors, and negative $\Delta\alpha$ by blue colors. On the diagonal we observe three positive–negative couplets when ν_{pump} is resonant with one of the three absorption bands. The negative $\Delta\alpha$ feature is due to the $\nu = 0 \rightarrow 1$ bleaching and $\nu = 1 \rightarrow 0$ stimulated emission of the excited vibrational mode, and the positive $\Delta\alpha$ feature is due to $\nu = 1 \rightarrow 2$ excited-state absorption, which is decreased in frequency with respect to the $\nu = 0 \rightarrow 1$ frequency as a consequence of the anharmonicity of the CO-stretch potential.

Strong cross peaks are observed between the B_1 peak and the $B_2/A_1^{(1)}$ peak, and weaker cross-peak features are observed between the B_1 and $A_1^{(2)}$ peaks and between the $B_2/A_1^{(1)}$ and $A_1^{(2)}$ peaks. Like the diagonal peaks, the cross peaks are doublets. This is because the cross peaks arise from a small decrease in frequency of the probed mode upon excitation of the pumped mode.[32] Since the diagonal anharmonicity (the difference between the $\nu = 0 \rightarrow 1$ and $\nu = 1 \rightarrow 2$ frequencies of a mode) and the cross anharmonicities (the lowering of $\nu = 0 \rightarrow 1$ frequency of a mode upon excitation of another mode that is coupled to it) are both comparable to, or smaller than the width of the absorption bands, the absorption-difference spectrum is very similar to the derivative of the absorption band with respect to the probe frequency, for both the diagonal peaks and the cross peaks.

The cross-peak anisotropies (see Fig. 3) are in agreement with the above-described assignment of the four normal modes. In a perfectly symmetric $Fe(CO)_4$(olefin) complex, the transition-dipole moments of the $A_1^{(1)}$, $B_1^{(1)}$, and $B_2^{(1)}$ modes are mutually perpendicular, and those of the $A_1^{(1)}$ and $A_1^{(2)}$ modes parallel. Since the anisotropy of a cross peak between two modes with perpendicular transition-dipole moments is −0.2, and that of a cross peak between two modes with parallel transition-dipole moments +0.4,[32] one would ideally expect to observe anisotropies of −0.2 for each of the cross peaks between the $A_1^{(1)}$, $A_1^{(2)}$, $B_1^{(1)}$, and $B_2^{(1)}$ modes, except for the cross-peak between $A_1^{(1)}$ and $A_1^{(2)}$ which should have anisotropy +0.4. However, due to the overlap of the B_2 and $A_1^{(1)}$ absorption bands, the observed anisotropies of all cross peaks involving either the B_2 or $A_1^{(1)}$ mode are not straightforward to interpret, since in this case two modes with perpendicular transition dipoles are simultaneously pumped or probed. For the remaining cross peaks, the deviations of the experimental anisotropies from the ideal ones are probably mainly caused by the distortion of the ideal trigonal bipyramid symmetry (due to the bulky and non-symmetric olefin),

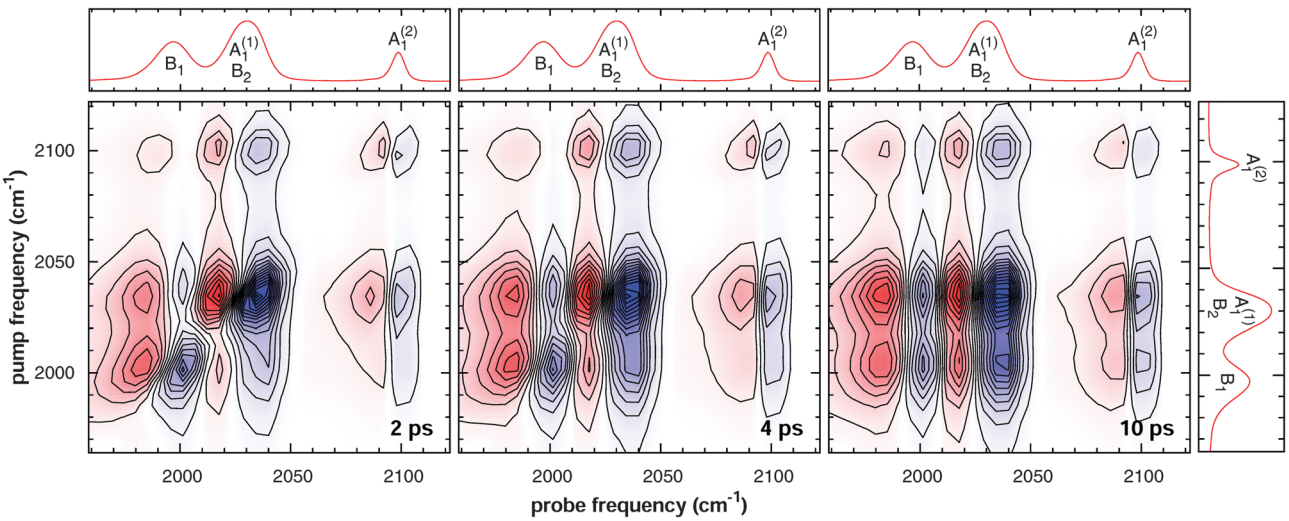

Fig. 2 2D spectra of $Fe(CO)_4$(cinnamic acid), showing the absorption change as a function of pump and probe frequency, from left to right for increasing waiting time between the pump and probe pulses (indicated in the bottom right corner of each plot). Blue denotes negative absorption change, red positive. The contour plots have been normalized to the maximum value of $\Delta\alpha$, resulting in a step size between consecutive contour levels of 6.2, 4.5 and 3.6 mOD for τ = 2, 4, and 10 ps, respectively.

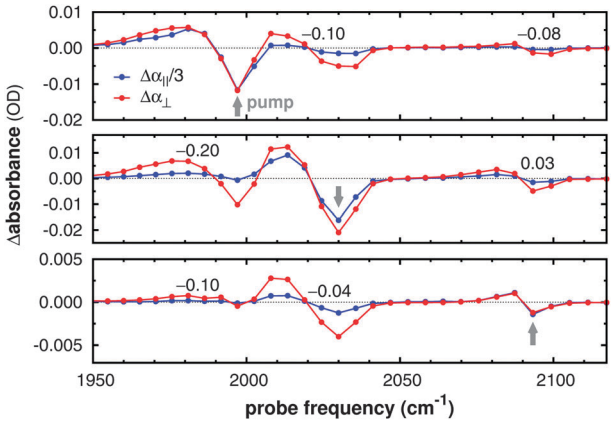

Fig. 3 Cross sections at three pump frequencies through the 2D spectrum of $Fe(CO)_4$(cinnamic acid) at τ = 2.5 ps, for parallel (blue points) and perpendicular (red points) polarizations of the pump and probe pulses. The measurements with parallel polarisation are scaled by a factor of 1/3 for better comparison. The cross-peak anisotropies are given above each cross peak.

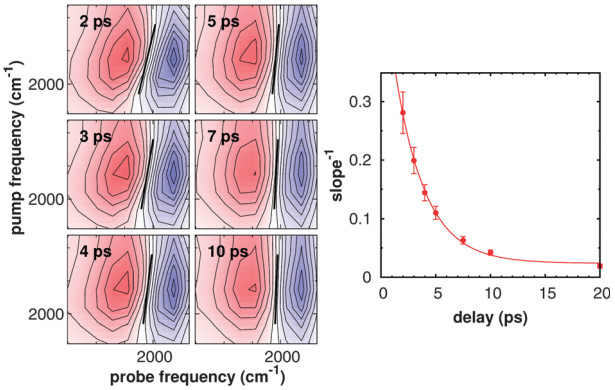

Fig. 5 Left: close-ups of the 2D-IR spectrum of $Fe(CO)_4$(dimethyl fumarate), showing the B_1 diagonal peak for several pump–probe delays. The solid lines show a least-squares fit to determine the slope of the diagonal peak at each delay value. Right: slope *vs.* pump–probe delay, together with a least-squares fit of an exponential fit, with τ_c = 2.8 ± 0.1 ps.

and perhaps partly by reorientation of the complex (the pump–probe delay time in these measurements was set to 2.5 ps).

3.3 Spectral fluctuations

At short delays, the contours of the peaks on the diagonal are slanted parallel to the diagonal, whereas at longer delays they become vertically aligned. This can be seen better in the close-ups shown in Fig. 4. The slope at short delay time shows that the absorption band is inhomogeneously broadened:[32] the response of the excited mode varies with the pump frequency. Frequency fluctuations scramble the inhomogeneity, and as a consequence at longer delays the response becomes increasingly independent of the pump frequency at which it has been excited. For sufficiently long delays, the response has become independent of the pump frequency and the 2D lineshapes are parallel to the pump-frequency axes. It can be shown that the slope of the diagonal is directly proportional to the frequency–frequency correlation function.[33] To determine the slope of the diagonal peak, we fit

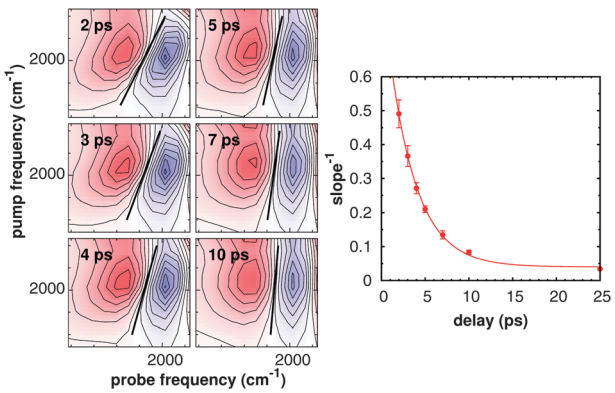

Fig. 4 Left: close-ups of the 2D-IR spectrum of $Fe(CO)_4$(cinnamic acid), showing the B_1 diagonal peak for several pump–probe delays. The solid lines show a least-squares fit to determine the slope of the diagonal peak at each delay value. Right: slope *vs.* pump–probe delay, together with a least-squares fit of an exponential fit, with τ_c = 3.1 ± 0.1 ps.

a straight line to the points where the $\Delta\alpha$ signals cross zero (the fits are shown as the black lines in the 2DIR spectra of Fig. 4). We find τ_c = 3.1 ± 0.1 ps and 2.8 ± 0.1 ps for $Fe(CO)_4$(cinnamic acid) and $Fe(CO)_4$(dimethyl fumarate), respectively (Fig. 5).

In contrast to the iron tetracarbonyl olefin complexes in chloroform solution studied here, inhomogeneous broadening is not observed in $Fe(CO)_5$ in *n*-dodecane, even at short delays after vibrational excitation.[2] This difference is probably due to the stronger interaction of the complex with the solvent (chloroform *vs. n*-dodecane) in our experiment. Previous 2D-IR studies on the rhodium dicarbonylacetylacetonato complex[25] have shown that in hexane the CO-stretch absorption bands are homogeneously broadened, whereas in chloroform they are inhomogeneously broadened, with frequency–frequency correlation times very similar to the ones observed here. Additional inhomogenous broadening might result from the presence of the olefin ligand in our complex. The olefin is not strongly bound to the iron in both complexes (the iron tetracarbonyl olefin complexes are quite labile[29]). Interactions with the solvent will therefore cause random fluctuations of the geometry between the olefin ligand and the metal center. This modulates the degree of pi-backbonding between the metal and its ligands, which translates into fluctuations of the C≡O bond strength. The slope of the diagonal peaks at 2 ps is greater in the $Fe(CO)_4$(cinnamic acid) complex which indicates greater inhomogeneity of the system as compared to the $Fe(CO)_4$(dimethyl fumarate) complex. As stated above, dimethyl fumarate is more strongly bound to the metal center than cinnamic acid and is therefore less affected by the fluctuations responsible for the inhomogeneous broadening.

3.4 Cross-peak dynamics

With increasing delay between the pump and probe pulses, the overall intensity of the 2D spectrum decreases on a time scale of tens of picoseconds. This is a consequence of $v = 1 \rightarrow 0$ population relaxation, which occurs with a time constant T_1 of ~60 ps (see ESI†). In addition to this overall intensity decay, the relative intensities of the diagonal and cross peaks also

change with increasing waiting time. At longer waiting times (middle and right panels of Fig. 2), the intensity of all the cross-peak features increases relative to the diagonal peak intensities. This is a consequence of transfer of the CO-stretch vibrational excitation between the different modes: if a particular mode X is excited by the pump pulse, and subsequently transfer of the excitation to mode Y occurs, this shows up as a decrease of the diagonal peak at $(\nu_{probe},\nu_{pump}) = (\nu_X,\nu_X)$, and a simultaneous increase of the cross-peak intensity at $(\nu_{probe},\nu_{pump}) = (\nu_Y,\nu_X)$. This can be seen to occur for all pairs of modes in Fig. 2 except the pair $B_2/A_1^{(1)}$ and $A_1^{(2)}$. The transfer of the excitation between the modes occurs on a time scale on the order of 10 ps, so that after 30 ps the transient absorption spectrum has become independent of the initially excited mode. This is clearly seen in cross sections through the 2D plots at different pump frequencies, shown in Fig. 6. The delay-time dependence of the cross peaks is not the same, see Fig. 7, where we show the intensity of the cross and diagonal peaks for three different pump frequencies (to get optimal estimates for the cross-peak and diagonal-peak amplitudes, we plot for each peak the difference of the negative and positive extrema *vs.* delay). These measurements were performed with the polarizations of pump and probe set at the magic angle (54.7°) with respect to each other in order to avoid effects of molecular reorientation on the data. After excitation of the B_1 mode at 1998 cm^{-1}, the intensities of the two cross peaks due to the $B_2/A_1^{(1)}$ and $A_1^{(2)}$ bands both increase with delay time, indicating that the excitation is transferred from B_1 to the other modes. Similar growth is observed for the B_1 mode after exciting either the $B_2/A_1^{(1)}$ or the $A_1^{(2)}$ band. Simultaneously with the growth of the cross peaks, the diagonal peaks show a decay on a similar time scale. In addition there is a slower overall decay of the signal due to population T_1 relaxation, which occurs with a time constant of ~60 ps (see ESI†). The cross peaks between the $B_2/A_1^{(1)}$ and $A_1^{(2)}$ bands show a decay rather than a growth.

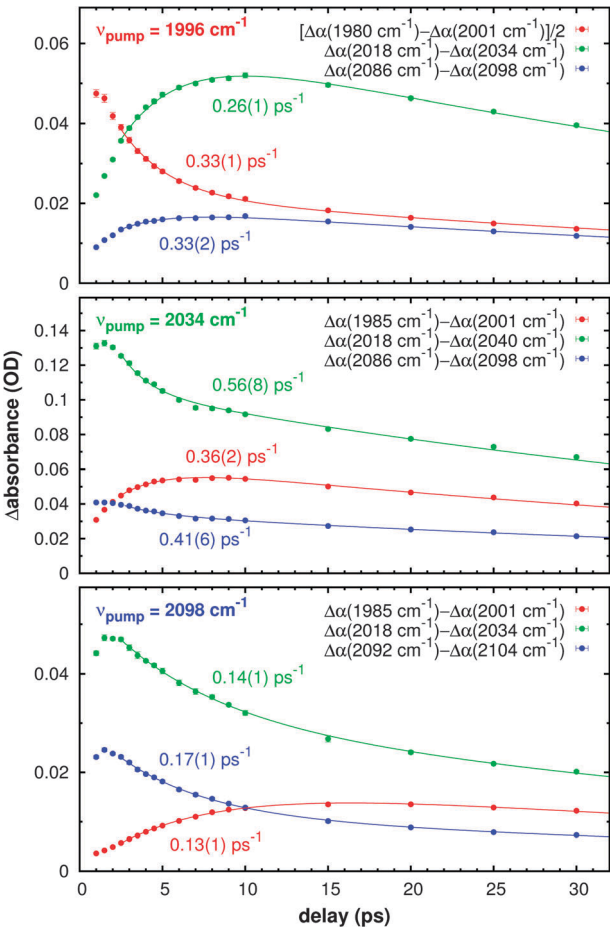

Fig. 7 Delay dependence of the cross-peak intensities observed in $Fe(CO)_4$(cinnamic acid), for three different pump frequencies (indicated at the left top of each plot), with the pump and probe polarizations at the magic angle. The cross-peak intensities are determined by taking the difference between their positive and negative extrema (the frequencies of which are indicated in the legend). The curves are biexponentials, with one fixed rate constant $1/T_1$ = 1/59 ps and a free rate constant, visible next to each curve.

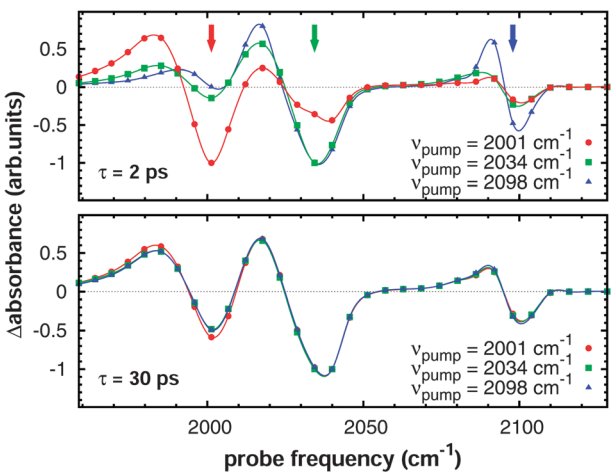

Fig. 6 Cross sections through the 2D spectrum of $Fe(CO)_4$(cinnamic acid) at pump–probe delays of τ = 2 ps (upper panel) and 30 ps (lower panel). For both delay values the signals have been scaled for better comparison. At a delay of 30 ps the signal has become independent of the pump frequency due to equilibration of the vibrational excitation over the four CO-stretching modes.

To characterize the cross-peak dynamics quantitatively we applied a singular-value decomposition[34,35] to the data. We find that the data are characterized by three kinetic components. One of these is the T_1 decay, so that the exchange kinetics is characterized by two kinetic components. From least-squares fits to the data shown in Fig. 7 (the fits are represented by the curves), we find that the exchange kinetics for each combination of pump and probe frequencies can be well described by a bi-exponential function, in which one of the two rate constants is the vibrational lifetime T_1 and the other varies between 0.1 and 0.6 ps^{-1} (the values are indicated in Fig. 7).

The short-time ($\tau < 10$ ps) delay dependence of the diagonal and cross peaks is caused by a redistribution of the CO-stretching excitations over the different modes, from the initially excited mode (giving a rise to a faster decay of the diagonal peak) to the other modes (giving rise to a growth of the cross peaks). Relaxation of the $v = 1$ excitation to the vibrational ground state occurs on a much slower time scale, and dominates the delay dependence for $\tau > 10$ ps.

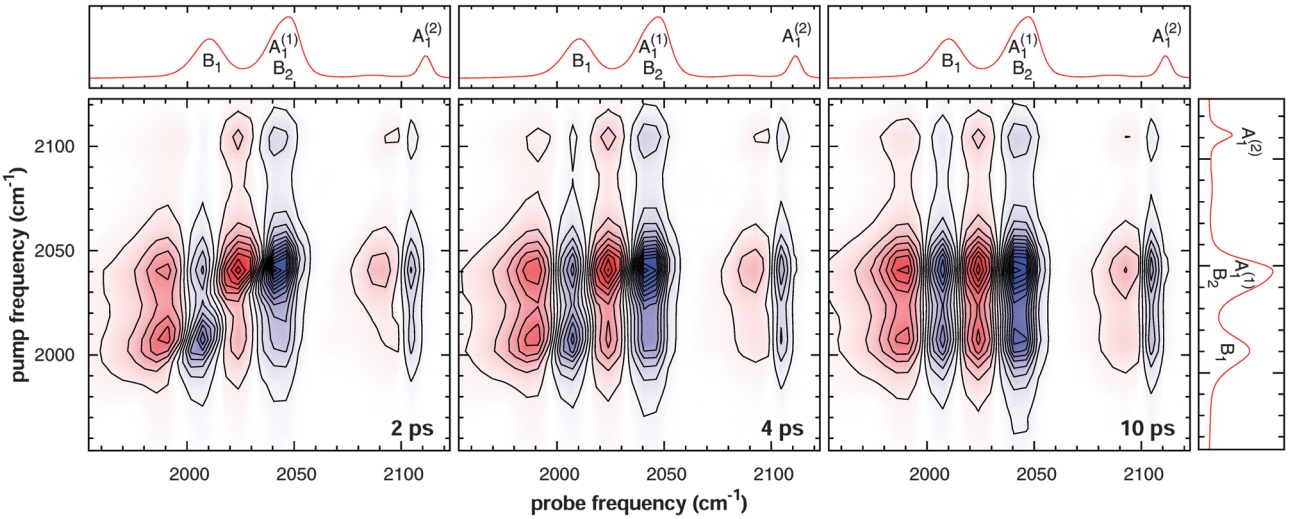

Fig. 8 2D spectra of $Fe(CO)_4$(dimethyl fumarate), showing the absorption change as a function of pump and probe frequency, from left to right for increasing waiting time between the pump and probe pulses (indicated in the bottom right corner of each plot). Blue denotes negative absorption change, red positive. The contour plots have been normalized to the maximum value of $\Delta\alpha$, resulting in a step size between consecutive contour levels of 6.2, 4.5 and 3.6 mOD for τ = 2, 4, and 10 ps, respectively.

3.5 Fluxionality or intramolecular vibrational relaxation?

The observed redistribution of the CO-stretch excitation can have two causes: a fluxional rearrangement of the ligands,[2] or a transfer of the excitation between the normal modes.[12] The effects can contribute simultaneously, but one might expect that in many cases one of the two dominates. The fluxional rearrangement involves a Berry pseudo-rotation in which the equatorial and axial CO ligands are exchanged.[30] Vibrational excitations on CO ligands are preserved during fluxional rearrangement.[2] Therefore, a complex in which a normal mode involving axial CO ligands is excited can rearrange to form a complex in which a normal mode involving equatorial ligands is excited, and *vice versa*. The fluxionality of the $Fe(CO)_4$(olefin) complexes is a two-state process with identical initial and final states, and therefore characterized by a single rate constant (the number of fluxional rearrangements per second). As a consequence, if fluxionality is the only process causing exhange of vibrational excitations, only a single rate constant should be observed in the exchange kinetics (in addition, there will be an overall decay due to T_1 relaxation, on a much slower time scale).

The exchange kinetics observed in the $Fe(CO)_4$(cinnamic acid) complex involves more than one time constant. This means that fluxionality cannot be the only cause of the observed kinetics, and that transfer of the vibrational excitation must play a role. The equilibration kinetics due to energy transfer between 4 normal modes involves at most 3 time constants. This can be understood as follows. Since there are four modes, the kinetics of excitation transfer between these modes is characterized by a set of 4 linear differential equations. This set of equations is determined by a 4 × 4 rate-constant matrix, which contains the rates $k_{i\rightarrow j}$ of energy transfer from state i to j. To solve the equations, one diagonalizes the matrix. In the case of population transfer, one of the eigenvalues is always 0 (the corresponding eigenvector being the sum of the 4 populations, which is conserved, and hence has a decay rate constant of zero). The other three eigenvalues are the rate constants observed in any population equilibration process of the 4-state system (the coefficients of the exponentials are determined by the initial conditions). Their values are complicated functions of the underlying rate constants $k_{i\rightarrow j}$. It is easily shown that the only effect of a finite T_1 is multiplication of all four populations by a factor $\exp(-t/T_1)$,‡ which represents the overall decay of the signal due to population relaxation to the vibrational ground state. If some of the underlying time constants $k_{i\rightarrow j}$ are either effectively zero (much smaller than the T_1 relaxation rate, and therefore not observable) or much faster than the experimental time resolution, or if some rate constants are equal, the observed kinetics can involve less than 3 time constants.

In the present case the observed exchange kinetics involves at least three rate constants (in addition to the overall, slow T_1 decay), so that two explanations are possible: a combination of fluxionality and energy transfer, or only energy transfer and very slow (*i.e.* slower than T_1, and hence not observable) fluxionality. To find out which of these explanations holds, we compare the dynamics of $Fe(CO)_4$(cinnamic acid) with that of $Fe(CO)_4$(dimethyl fumarate). The fluxionality of $Fe(CO)_4$(dimethyl fumarate) is much slower than in $Fe(CO)_4$(cinnamic acid). In an NMR study on a series of iron tetracarbonyl olefin complexes, fluxionality was found to be related to the ability of the olefin to rotate with respect to the complex,[36] because the orientation of the olefin along the CO-axial axis is energetically not favored. If pi-backbonding is strong between the metal and the olefin, the energy barrier for olefin rotation is higher, resulting in a slower rate of fluxionality. Accordingly, tetracarbonyl(styrene)-iron exhibits only one coalesced ^{13}C peak down to 193 K,

‡ In that case, the rate equations for the time derivatives of the populations $\dot{n}_i$ all have an additional loss term $-n_i/T_1$, which can be eliminated by substituting $n_i(t) = n_i^0(t)\exp(-t/T_1)$. The rate equations for the time derivatives of the renormalized populations n_i^0 are the same as the ones for $\dot{n}_i$ with infinite T_1.

indicating that the fluxional behavior is too fast even at this low temperature to be observable on the NMR time scale. For tetracarbonyl(dimethyl fumarate)iron the rate of fluxional rearrangement is 85 ± 2 s^{-1} at 263 K.[36] The different rates of fluxionality can be explained using the Dewar–Chatt–Duncanson model.[37,38] Pi-backbonding to the dimethyl fumarate ligand is stronger than to styrene, because the ester substituents of the former inductively remove electron density from the π* orbital of the double bond. This results in a lowering of the energy of the π* orbital which in turn improves overlap with the d orbitals of the metal. The bonding between the metal centre and olefin ligands with a higher degree of pi-backbonding takes on character of a metallocyclopropane. In this species, both carbon atoms form bonds with the metal center. This is not conducive to rotation along the binding axis, hence the rate of fluxionality of $Fe(CO)_4$(dimethyl fumarate) should be much slower than that of $Fe(CO)_4$(cinnamic acid). Taking into account that vibrational energy transfer is insensitive to the nature of the olefin ligand, comparing these two complexes makes it possible to determine the contribution of fluxionality to the observed cross-peak dynamics.

Fig. 8 shows the 2D-IR spectrum of $Fe(CO)_4$(dimethyl fumarate) for several pump–probe delay values. Apart from the overall shift of the CO-stretch frequencies due to the stronger binding of the olefin ligand (explained above), these 2D-IR spectra are essentially identical to those of $Fe(CO)_4$(cinnamic acid). The cross-peak dynamics of $Fe(CO)_4$(dimethyl fumarate), shown in Fig. 9, is also very similar to that observed in $Fe(CO)_4$(cinnamic acid). In particular, from a singular-value decomposition of the delay-dependent data we find again that the kinetics is characterized by three components (see ESI†). The rate constants of the exchange kinetics are very similar to those of $Fe(CO)_4$(cinnamic acid) (see Fig. 9). On the other hand, because of stronger pi-backbonding of dimethyl fumarate as compared to cinnamic acid, the rate of fluxionality is much slower in $Fe(CO)_4$(dimethyl fumarate) than in $Fe(CO)_4$(cinnamic acid). From the fact that no essential difference is observed in the cross-peak kinetics of the complexes, we can conclude that fluxionality makes no significant contribution to the cross-peak dynamics in $Fe(CO)_4$(olefin) complexes.

The underlying kinetic parameters are the rates $k_{i\rightarrow j}$ of energy transfer from state i to j. The 4 × 4 exchange-rate constant matrix contains 12 transfer rates, but due to the requirement of detailed balance the number of unknown rates reduces to 6. It is unfortunately not possible to determine these underlying rates from our experimental results. Such an analysis involves solving the 4 rate equations for different initial conditions (determined by the pump frequency), and performing a global fit of the solution to the 2D data set. There are two complications: (1) if modes A and B are coupled, a cross peak at $(\nu_{probe},\nu_{pump}) = (\nu_B,\nu_A)$ shows delay dependence not only due to a change in the population of mode B upon exciting mode A, but also due to a change in the population of mode A; for instance, energy transfer from modes A to C will lead to a decrease of the cross peak (ν_B,ν_A). The relation between populations and cross peaks is a linear transformation, and thus determined by a 4 × 4 matrix. This complication can in principle be solved by accurately determining the numbers in this matrix from the cross-peak intensities at $\tau = 0$. (2) However, since the bands of the B_2 and $A_1^{(1)}$ modes overlap completely, such an approach is not feasible in this particular case. The problem of obtaining the transfer rates from the observed cross-peak dynamics is therefore underdetermined.

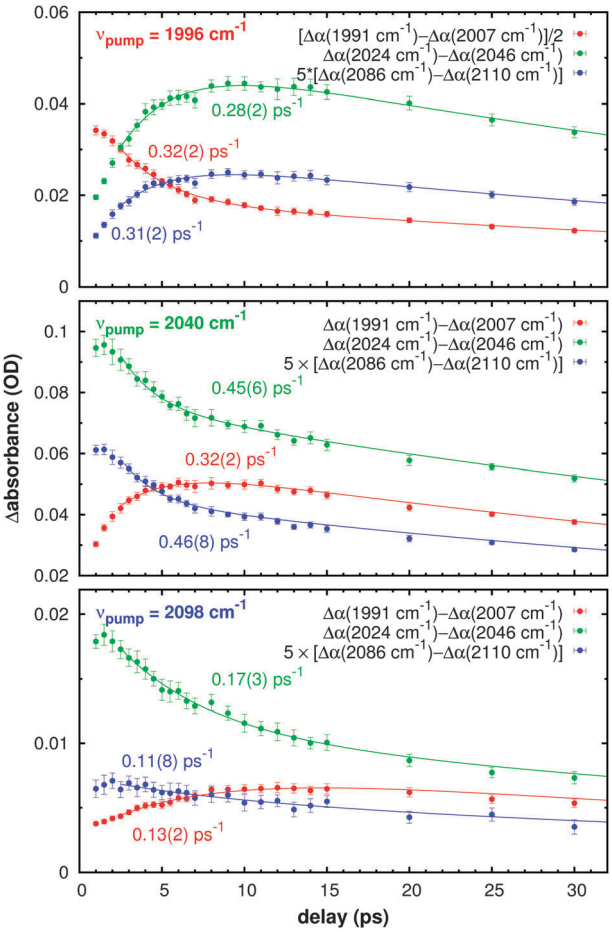

Fig. 9 Delay dependence of the cross-peak intensities observed in $Fe(CO)_4$(dimethyl fumarate), for three different pump frequencies (indicated at the left top of each plot), with the pump and probe polarizations at the magic angle. The cross-peak intensities are determined by taking the difference between their positive and negative extrema (the frequencies of which are indicated in the legend). The curves are biexponentials, with one fixed rate constant $1/T_1$ = 1/67 ps and a free rate constant, visible next to each curve.

Unlike previously investigated iron carbonyl complexes,[2,5] those investigated here exhibit IVR on the picosecond time scale. This difference is probably due to the stronger interaction with the solvent, and to the presence of the olefin ligand. Energy transfer between the CO-stretch modes occurs only if the modes are coupled, and is caused by fluctuations of the frequencies and/or of the coupling between the modes.[32,39,40] As discussed above, the conformation of the olefin ligand with respect to the rest of the iron complex fluctuates due to interaction with the solvent, and these fluctuations cause fluctuations of both the CO-stretch frequencies and the couplings, in addition to the fluctuations caused by direct interaction of the CO ligands with the solvent. The intense cross peaks at early delays after vibrational excitation observed in the 2D-IR spectra of both iron tetracarbonyl olefin complexes indicate that coupling between the vibrational modes

is much stronger than in $Fe(CO)_5$. The combination of this strong coupling and the strong interaction with the solvent gives rise to the fast IVR observed in our experiments.

4 Conclusion

We find that redistribution of CO-stretch vibrational excitations between the four CO-stretch modes of $Fe(CO)_4$(cinnamic acid) and $Fe(CO)_4$(dimethyl fumarate) occurs on the picosecond time scale, with characteristic time constants between 2 and 10 ps. The spectral fluctuations of the normal modes are found to occur on a similar time scale ($\sim$3 ps). From the comparison of $Fe(CO)_4$(cinnamic acid) and $Fe(CO)_4$(dimethyl fumarate) we can conclude that no fluxionality occurs in these complexes on the investigated time scale (up to tens of ps), in contrast to iron-tricarbonyl complexes (where fluxionality occurs with a time constant of 650 fs)[5] and ironpentacarbonyl complexes (where it occurs with a time constant of 8 ps).[2] The strong vibrational coupling between the carbonyl stretch modes combined with the strong solute–solvent interactions and the sensitivity of the olefin ligand to solvent fluctuations in the iron tetracarbonyl olefin complexes studied here, results in the observed fast IVR.

Acknowledgements

The authors thank Hans Sanders for valuable discussions. This work was supported by the Stichting voor Fundamenteel Onderzoek der Materie (FOM) which is financially supported by the Nederlandse Organisatie voor Wetenschappelijk Onderzoek (NWO).

References

1 P. W. van Leeuwen, *Homogeneous Catalysis Understanding the Art*, Kluwer Academic Publishers, 2004.
2 J. F. Cahoon, K. R. Sawyer, J. P. Schlegel and C. B. Harris, *Science*, 2008, **319**, 1820–1823.
3 C. B. Harris, R. M. Shelby and P. A. Cornelius, *Chem. Phys. Lett.*, 1978, **57**, 8–14.
4 R. M. Shelby, C. B. Harris and P. A. Cornelius, *J. Chem. Phys.*, 1979, **70**, 34–41.
5 F.-W. Grevels, K. Kerpen, W. E. Klotzbücher, R. E. D. McClung, G. Russell, M. Viotte and K. Schaffner, *J. Am. Chem. Soc.*, 1998, **120**, 10423–10433.
6 C. H. Londergan and C. P. Kubiak, *Chem.–Eur. J.*, 2003, **9**, 5962–5969.
7 S. Mukamel, *Annu. Rev. Phys. Chem.*, 2000, **51**, 691–729.
8 P. Hamm, M. Lim and R. M. Hochstrasser, *J. Phys. Chem. B*, 1998, **102**, 6123–6138.
9 D. M. Jonas, *Annu. Rev. Phys. Chem.*, 2003, **54**, 425–463.
10 M. Cho, *Chem. Rev.*, 2008, **108**, 1331–1418.
11 W. T. Grubbs, T. P. Dougherty and E. J. Heilweil, *Chem. Phys. Lett.*, 1994, **227**, 480–484.
12 O. Golonzka, M. Khalil, N. Demirdöven and A. Tokmakoff, *J. Chem. Phys.*, 2001, **115**, 10814–10828.
13 J. Bredenbeck, J. Helbing, R. Behrendt, C. Renner, L. Moroder, J. Wachtveitl and P. Hamm, *J. Phys. Chem. B*, 2003, **107**, 8654–8660.
14 J. Bredenbeck, J. Helbing and P. Ham, *J. Chem. Phys.*, 2004, **121**, 5943–5957.
15 J. Bredenbeck, J. Helbing and P. Hamm, *J. Am. Chem. Soc.*, 2004, **126**, 990–991.
16 A. I. Stewart, I. P. Clark, M. Towrie, S. K. Ibrahim, A. W. Parker, C. J. Pickett and N. T. Hunt, *J. Phys. Chem. B*, 2008, **112**, 10023–10032.
17 C. R. Baiz, P. L. McRobbie, J. M. Anna, E. Geta and K. J. Kubarych, *Acc. Chem. Res.*, 2009, **42**, 1395–1404.
18 J. M. Anna, M. R. Ross and K. J. Kubarych, *J. Phys. Chem. A*, 2009, **113**, 6544–6547.
19 J. T. King, C. R. Baiz and K. J. Kubarych, *J. Phys. Chem. A*, 2010, **114**, 10590–10604.
20 S. Woutersen and P. Hamm, *Chem. Phys.*, 2001, **266**, 137–147.
21 J. Zheng, K. Kwak, J. Asbury, X. Chen, I. R. Piletic and M. D. Fayer, *Science*, 2005, **309**, 1338–1343.
22 Y. S. Kim and R. M. Hochstrasser, *Proc. Natl. Acad. Sci. U. S. A.*, 2005, **102**, 11185–11190.
23 J. Bredenbeck, J. Helbing, C. Kolano and P. Hamm, *ChemPhysChem*, 2007, **8**, 1747–1756.
24 V. M. Kenkre, A. Tokmakoff and M. D. Fayer, *J. Chem. Phys.*, 1994, **101**, 10618–10629.
25 M. Khalil, M. Demirdöven and A. Tokmakoff, *J. Phys. Chem. A*, 2003, **107**, 5258–5279.
26 M. Khalil, M. Demirdöven and A. Tokmakoff, *J. Chem. Phys.*, 2004, **121**, 362–373.
27 J. M. Anna and K. J. Kubarych, *J. Chem. Phys.*, 2010, **133**, 174506.
28 A. Huerta-Viga, D. J. Shaw and S. Woutersen, *J. Phys. Chem. B*, 2010, **114**, 15212–15220.
29 E. Weiss, K. Stark, J. E. Lancaster and H. D. Murdoch, *Helv. Chim. Acta*, 1958, **62**, 288–297.
30 T. A. Albright, R. Hoffman, J. C. Thibeault and D. L. Thorn, *J. Am. Chem. Soc.*, 1979, **101**, 3801–3812.
31 D. J. Darensbrough, H. H. Nelson and C. L. Hyde, *Inorg. Chem.*, 1974, **13**, 2135–2145.
32 P. Hamm and M. T. Zanni, *Concepts and Methods of 2D Infrared Spectroscopy*, Cambridge University Press, 2011.
33 K. Kwac and M. Cho, *J. Chem. Phys.*, 2003, **119**, 2256–2263.
34 W. H. Press, S. A. Teukolsky, W. T. Vetterling and B. P. Flannery, *Numerical Recipes in C*, Cambridge University Press, Cambridge, UK, 1992.
35 M. R. Panman, P. Bodis, D. J. Shaw, B. H. Bakker, A. C. Newton, E. R. Kay, D. A. Leigh, W. J. Buma, A. M. Brouwer and S. Woutersen, *Phys. Chem. Chem. Phys.*, 2012, **6**, 1865–1875.
36 S. T. Wilson, N. J. Corville, J. R. Shapely and J. A. Osborn, *J. Am. Chem. Soc.*, 1974, **96**, 4038–4040.
37 M. Dewar, *Bull. Soc. Chim. Fr.*, 1951, C79.
38 J. Chatt and L. Duncanson, *J. Chem. Soc.*, 1953, 2939–2947.
39 R. J. Abbott and D. W. Oxtoby, *J. Chem. Phys.*, 1980, **72**, 3972–3978.
40 S. Woutersen, Y. Mu, G. Stock and P. Hamm, *Proc. Natl. Acad. Sci. U. S. A.*, 2001, **98**, 11254–11258.

